MOLECULAR BIOLOGY

EF-G–induced ribosome sliding along the noncoding mRNA

M. Klimova*, T. Senyushkina*, E. Samatova*, B. Z. Peng, M. Pearson, F. Peske, M. V. Rodnina†

Translational bypassing is a recoding event during which ribosomes slide over a noncoding region of the messenger RNA (mRNA) to synthesize one protein from two discontinuous reading frames. Structures in the mRNA orchestrate forward movement of the ribosome, but what causes ribosomes to start sliding remains unclear. Here, we show that elongation factor G (EF-G) triggers ribosome take-off by a pseudotranslocation event using a small mRNA stem-loop as an A-site transfer RNA mimic and requires hydrolysis of about two molecules of guanosine 5′-triphosphate per nucleotide of the noncoding gap. Bypassing ribosomes adopt a hyper-rotated conformation, also observed with ribosomes stalled by the SecM sequence, suggesting common ribosome dynamics during translation stalling. Our results demonstrate a new function of EF-G in promoting ribosome sliding along the mRNA, in contrast to codon-wise ribosome movement during canonical translation, and suggest a mechanism by which ribosomes could traverse untranslated parts of mRNAs.

INTRODUCTION

Translational bypassing has been described in bacteria and mitochondria of yeast *Magnusiomycetes* (*1*, *2*). The best-characterized example of bypassing is the gene *60* mRNA of bacteriophage T4 (*1*). The ribosome reads the first 46 mRNA codons of the open reading frame (ORF) up to the GGA triplet coding for amino acid glycine. The subsequent codon is stop codon UAG (Fig. 1A), but instead of terminating protein synthesis, the ribosome slides over a 50–nucleotide (nt)–long noncoding gap, lands at a distal GGA codon, and resumes translation to the end of the second ORF. Although all ribosomes disengage from the take-off GGA codon and start sliding, only 50 to 60% of them synthesize the full-length protein, while the remaining ribosomes stop translation due to termination or the spontaneous drop-off of the peptidyl-tRNA^{Gly} (*3*–*5*).

Gene *60* mRNA elements that stimulate bypassing are located 5′ of the take-off site, in the take-off stem-loop (SL), and 3′ of the landing site (*1*, *3*, *5*–*7*). The roles of the 5′SL and 3′SL are to promote directionality of movement and to ensure correct landing, respectively (*3*, *5*). The role of the take-off SL is less clear, although it is critical for bypassing (*1*, *5*, *8*). A recent cryogenic electron microscopy (cryo-EM) structure revealed that, in the state stalled before bypassing, the mRNA folds into a short dynamic SL that occupies the decoding site of the small ribosomal subunit (*6*). The A-site SL could induce a lateral tension on the mRNA–transfer RNA (tRNA) interaction, which would cause the disengagement of the anticodon-codon interaction (*5*); however, the cryo-EM structure shows that the interactions of the peptidyl-tRNA^{Gly} anticodon with the mRNA codon and the P site of the ribosome remain intact and there is no visible tension in the complex (*6*). The short SL hinders the access of the translation termination factor or near-cognate aminoacyl-tRNA into the A site, thereby protecting the bypassing ribosomes from termination or read-through (*6*).

Another prominent feature of the take-off complex is the nascent peptide, which forms numerous interactions with the ribosome tunnel (*6*). The interactions stabilize the binding of the peptidyl-tRNA^{Gly} to the ribosome during sliding. In addition, the contacts of the nascent peptide residues in the vicinity of the peptidyl transferase center stabilize its inactive conformation, which provides an additional mechanism to prevent the premature termination and read-through. In the take-off complex, the ribosome adopts a rolled conformation, which is also found in other stalled complexes (*6*, *9*). In contrast to normal translation, where ribosomes move by one codon at a time, during bypassing, the ribosome slides over the mRNA. A similar type of ribosome movement has been recently described in 3′ untranslated regions of eukaryotic mRNAs, where ribosome profiling identified nontranslating ribosomes that slide along the mRNA (*10*, *11*), but the mechanism is not known. It is also not known how the ribosome deals with an SL structure in the A site before sliding. Last, it remains unclear how ribosome dynamics is connected to sliding and whether the movements are similar to other stalled complexes. Here, we address these questions by a combination of biochemical and single-molecule total internal reflection fluorescence (TIRF) approaches.

RESULTS

Elongation factor G promotes bypassing at the cost of guanosine 5′-triphosphate hydrolysis

To identify what triggers bypassing, we used the fully reconstituted translation system, which functions with the speed and accuracy comparable to those in vivo (*12*, *13*). The bypassing efficiency on a full-length gene *60* is ~60% (Fig. 1B). At low temperatures (4° to 10°C), ORF1 is translated, but the bypassing product is not formed. Upon temperature shift to 37°C, the ribosomes resume bypassing (Fig. 1C) (*6*). Those ribosomes that landed at the GGA codon at the beginning of the second ORF read a leucine codon UUA when resuming translation (Fig. 1A); hence, we used [^{14}C]Leu incorporation into the nascent peptide as a readout for bypassing (Fig. 1D and fig. S1). Raising the temperature and addition of EF-Tu–GTP–[^{14}C]Leu-tRNA alone do not result in productive bypassing. Ribosomes incorporate [^{14}C]Leu only when elongation factor G (EF-G) is present in the reaction mixture, suggesting that bypassing is triggered by EF-G. EF-G variants with mutations H583K or Q507D in its

Max Planck Institute for Biophysical Chemistry, Department of Physical Biochemistry, 37077 Göttingen, Germany.
*These authors contributed equally to this work.
†Corresponding author. Email: rodnina@mpibpc.mpg.de

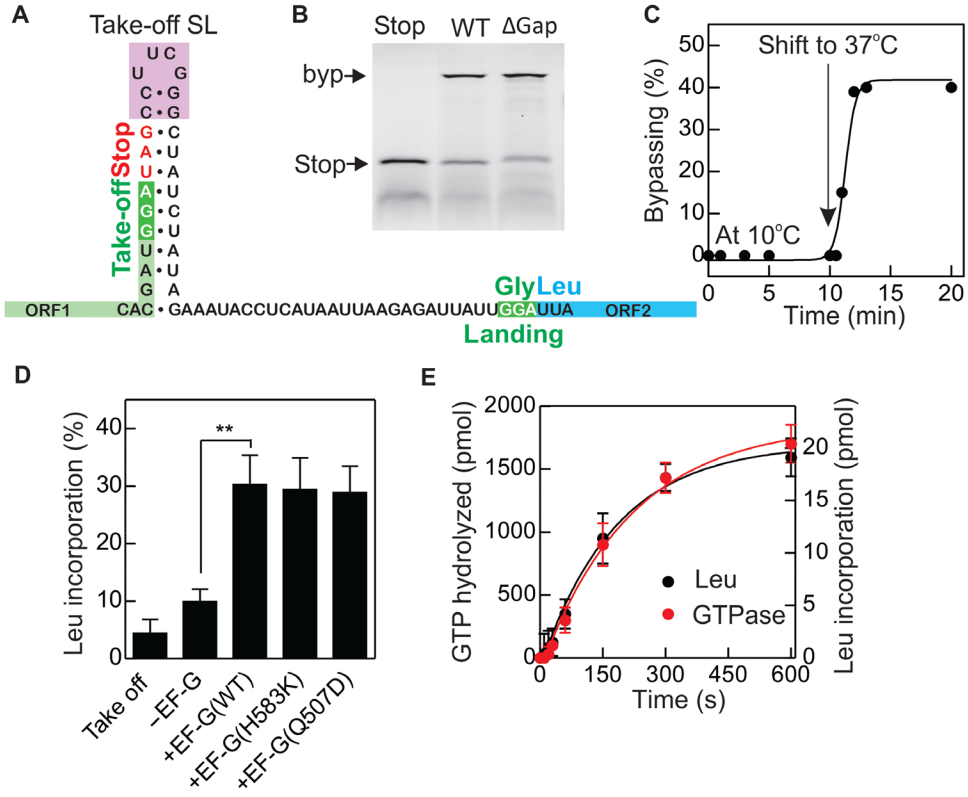

Fig. 1. EF-G initiates translational bypassing. (**A**) Schematic of the gene *60* mRNA. ORF1 (light green) spans codons 1 to 46 up to the Gly take-off codon, GGA (green), followed by a UAG stop codon (red). ORF2 (blue) begins with a Leu codon UUA after the landing codon (green) (*1*, *3*). (**B**) The translation products of gene *60* visualized using a fluorescent reporter, BODIPY FL, incorporated cotranslationally at the N terminus of the nascent peptide (*3*). mRNA constructs that code for ORF1 alone (stop), the full-length protein consisting of ORF1+ORF2 separated by a noncoding gap (WT), or the full-length protein synthesized as a single ORF1+ORF2 polypeptide without the gap (Δgap). The short peptide corresponds to amino acids 1 to 46 (stop); bypassing results in a 160 amino acids long product that includes the second ORF (byp). (**C**) Temperature dependence of bypassing. (**D**) Identification of the component that initiates bypassing. Take-off complexes were prepared and purified from translational components at 10°C and transferred to 37°C (take-off). In all other experiments, EF-Tu–GTP–[^{14}C]Leu-tRNA was added in the absence of EF-G (–EF-G) or in the presence of EF-G(WT), EF-G with mutations in domain 4 [+EF-G(H583K) and +EF-G(Q507D)]. Error bars show the SD for $n = 3$ replicates. $^{**}P < 0.005$ by Student's two-tailed unpaired t test. (**E**) Guanosine triphosphatase (GTPase) activity of EF-G during bypassing and the kinetics of bypassing measured by [^{14}C]Leu incorporation. Error bars show the SD for $n = 3$ replicates.

domain 4, which slow down the canonical tRNA-mRNA translocation (*14*), can also promote bypassing.

To test whether the role of EF-G is limited to a single action in triggering sliding, we measured guanosine 5′-triphosphate (GTP) hydrolysis by EF-G during bypassing and compared it to the kinetics of bypassing as reported by [^{14}C]Leu incorporation (Fig. 1E). EF-G alone does not hydrolyze GTP; the reaction is activated by the interaction with the ribosome. During canonical translocation, EF-G hydrolyzes about one GTP molecule each time the ribosome moves by one codon. However, the factor can also slowly hydrolyze GTP uncoupled from movement, i.e., on vacant or stalled ribosomes. To account for the fraction of the ribosomes in the take-off complex that do not bypass, we compared GTP hydrolysis on bypassing ribosomes to that on the take-off complex in which bypassing is blocked by truncation of the mRNA downstream of the stop codon; the difference in GTP hydrolysis by bypassing and stalled ribosomes is shown in Fig. 1E. Bypassing ribosomes hydrolyze substantially more GTP than expected from a single take-off event based on the bypassing efficiency (Fig. 1E), indicating multiple EF-G binding/GTP hydrolysis events. The kinetics of GTP hydrolysis and bypassing are identical. The time courses are single exponential, suggesting a single rate-limiting step for GTP hydrolysis and bypassing. When normalized for the number of ribosomes that reach the landing site and assuming that GTP is hydrolyzed while the ribosome moves along the mRNA, EF-G appears to hydrolyze, on average, about 90 molecules of GTP for each ribosome that completed bypassing. Considering the length of the noncoding gap (50 nt), EF-G hydrolyzes, on average, 1.8 molecules of GTP per nucleotide of the sliding sequence. This GTP expenditure may be required to maintain the ribosome conformation that is prone to sliding or to facilitate the forward direction of sliding, similar to the power-stroke action of EF-G in translocation (*15*).

The role of the A-site mRNA SL element

We next asked the question whether the SL mRNA structure formed in the A site plays a role in initiating bypassing (Fig. 2A). We introduced mutations into the mRNA that either disrupt or stabilize base pairing in the hairpin and determined how these mutations affect bypassing efficiency in the translation assay (Fig. 2B). The stability of the SL mRNA element was calculated by mfold (http://unafold.rna.albany.edu/?q=mfold). Plotting the bypassing efficiency against the predicted folding energy shows a dose-dependent response with

the bypassing efficiency increasing with helix stability up to about −17 kcal/mol; further stabilization does not increase the bypassing efficiency (Fig. 2, B and C). Thus, a stable A-site hairpin is needed for efficient bypassing, which raises the question of what happens with a stable hairpin when the ribosome slides along the mRNA. We note that the A-site SL occupies the space where the tRNA anticodon domain is located during canonical translocation (*6*). It is possible that upon binding to the ribosome, EF-G domain 4 contacts the SL and promotes a partial translocation event by analogy with the translocation of the anticodon SL fragment of a tRNA (*16*). This model explains how the A-site SL could contribute to promoting disengagement of anticodon-codon interactions of the P-site $tRNA^{Gly}$ (*5*).

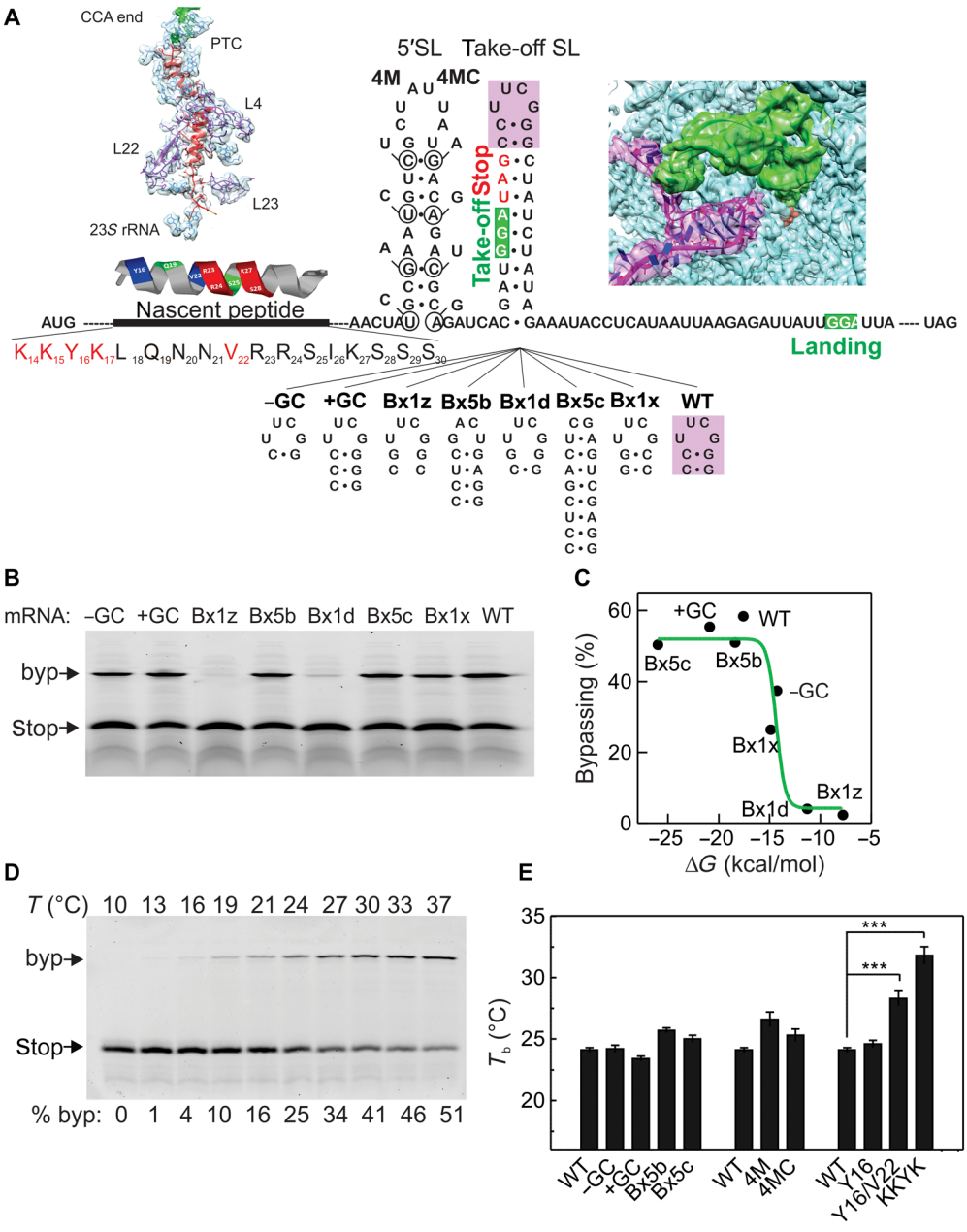

Fig. 2. The role of mRNA-encoded elements in initiating bypassing. (**A**) mRNA elements required for bypassing. The structure of the nascent peptide in the exit tunnel (left top inset) is from a cryo-EM structure (*6*). PTC, peptidyl transferase center of the ribosome. The schematic of the α-helical nascent peptide and the amino acid sequence indicated below show the positions (red) that affect bypassing (*3*). Circles in the 5′SL indicate mutations introduced to disrupt (4M) or to restore (4MC), the putative secondary structure of the 5′SL (*3*). The mutated part of the take-off SL is highlighted in pink; the mutations in the loop are shown below the mRNA sequence. The cryo-EM structure of the folded A-site SL (purple) and the P-site tRNA (green) within the ribosome (blue) (*6*) is shown in the right inset. (**B**) Effect of mutations in the apical part of the take-off SL on bypassing [nomenclature taken from (*1*)]. (**C**) Bypassing efficiency at predicted folding energies of the take-off SL variants. (**D**) Temperature dependence of bypassing. (**E**) Effect of mutations in the take-off SL, 5′SL, and the nascent peptide (Y16H, Y16H/V22D, and KKYK mutated to EEHE) on the temperature dependence of bypassing. Given is the temperature T_b at which bypassing is half-maximal. Error bars show the SD for $n = 3$ replicates. ***$P < 0.0005$ by Student's two-tailed unpaired t test.

The anticodon-codon interactions in the P site are destabilized by EF-G binding and translocation (*17*) and further by the departure of the tRNA from the E site (*5*), which could allow the ribosome to start sliding along the mRNA. However, in contrast to canonical translocation, the P-site peptidyl-tRNA remains attached to the ribosome due to interactions of the nascent peptide with the exit tunnel walls (*6*).

Conformational dynamics as modulator of bypassing

The bypassing efficiency increases with temperature (Fig. 2D). The temperature at which the bypassing efficiency is half of its maximum value, T_b, is 24.1° ± 0.2°C (Fig. 2E and fig. S2, B to D). The temperature dependence manifests a conformational transition that is crucial for bypassing, which prompted us to seek which element of the complex—mRNA, ribosome, or any other translational component—determines the temperature dependence. The folding-unfolding transitions of the mRNA elements would provide the simplest explanation for the observed temperature effect. However, mutations in the take-off or 5′SL do not affect the T_b value (Fig. 2E and fig. S2, B and C). Another important bypassing signal is provided by the interactions of the nascent peptide with the polypeptide exit tunnel of the ribosome (*3*, *5*, *6*). Replacement of residue Y16 to D (Y16D) or of the KKYK signature motif (amino acids 14 to 17) reduces bypassing [fig. S2A and (*3*)] but does not alter the temperature dependence (Fig. 2E and fig. S2D), whereas a double mutation Y16H/V22D shifts the T_b value substantially, from 24.1° to 28.3°C. Replacement of the entire KKYK motif with EEHE increases the T_b value markedly to 31.8°C.

The A site of the ribosome provides the environment for the presumed interactions between the mRNA take-off SL and the tip of EF-G domain 4, which prompted us to test how mutations in the ribosome decoding site and in EF-G affect the temperature sensitivity. Ribosomal protein S12 plays a key role in organizing the structure of the decoding site and controls aminoacyl-tRNA selection and tRNA translocation (*18*–*20*). We tested two S12 mutants with substitutions K42N or R49K. These amino acid residues are oriented toward the mRNA in the decoding center but do not affect canonical translocation (Fig. 3A and fig. S3, F and I). Mutations in S12, and in particular R49K, shift the T_b value toward lower temperatures; thus, the ribosomes show a relaxed phenotype that allows bypassing to occur at lower temperatures than with wild-type ribosomes (Fig. 3B and fig. S3, A to E). In contrast to S12 mutations, replacements of key amino acids at the tip of domain 4 of EF-G (H583K and Q507D), which are known to interact with the tRNA in the A site (*21*, *22*), shift the temperature dependence toward higher T_b values (Fig. 3B). Combining S12 and EF-G domain 4 mutations shows that a mutation in domain 4, such as Q507D, can suppress the relaxed phenotype of the S12 mutations. Thus, bypassing is sensitive to temperature-dependent conformational dynamics of the decoding center, with S12 restricting and EF-G promoting bypassing.

Dynamics of the ribosomes visualized by single-molecule fluorescence resonance energy transfer

Ribosomes stalled at the take-off site at low temperature adopt an unusual rolled conformation that differs from the classical nonrotated and rotated states sampled during regular translation (*6*). We asked whether this conformation is retained during bypassing. We monitored ribosome conformations using a single-molecule fluorescence resonance energy transfer (smFRET) technique. The small and large ribosomal subunits were labeled with Cy5 and Cy3, respectively, and the subunit rotation dynamics was monitored by smFRET between the two dyes (*23*–*27*). The two canonical conformations of the ribosome during translation, the nonrotated and rotated, correspond to FRET efficiencies of ~0.7 and ~0.5, respectively (*24*, *27*). The distance between the two reporters in the rolled and the nonrotated state is similar, and in fact, most of the stalled take-off complexes are in the FRET state of 0.7 at low temperature (Fig. 4A). At 22°C in the absence of EF-G, a new ribosome population appears with the FRET efficiency of 0.3, indicating a higher degree of subunit rotation than the canonical rotated state (Fig. 4B). The hyper-rotated intermediate was not captured in previous smFRET experiments (*5*), most likely due to a different FRET pair used in that study. After incubation with EF-G–GTP at 37°C, i.e., under conditions where bypassing is completed, ribosomes return to the rotated conformation (Fig. 4C). Addition of EF-Tu–GTP–Leu-tRNA^{Leu}, which leads to Leu incorporation into the nascent peptide and the next round of canonical translocation of the peptidyl-tRNA^{Leu} to the P site, brings the ribosome to the FRET state of 0.7, most likely the nonrotated, state (Fig. 4D). Time-resolved smFRET traces obtained upon addition of EF-G to the take-off complexes during imaging show transitions from the hyper-rotated to the rotated state (Fig. 4E), whereas transitions to and from the nonrotated state are not observed. This indicates that higher temperature activates ribosomes by promoting the formation of the hyper-rotated state and that the EF-G–dependent transition from the hyper-rotated to the rotated state is a hallmark of bypassing.

We then analyzed which elements of the bypassing complex are needed to promote the hyper-rotated state (Fig. 4F). To simplify the comparison, we normalized the data to show only the expected potentially active complexes (Fig. 1C). Of those, 80% adopt the hyper-rotated conformation at 22°C; after incubation with EF-G at 37°C, most complexes convert to the rotated state; addition of a large EF-G excess during imaging has no further effect, whereas the first round of translation of the second ORF brings about the nonrotated state. The formation of the hyper-rotated state depends not only on the temperature but also on the interactions of the nascent peptide with the exit tunnel and the presence of a stable take-off SL, as mutations in the KKYK motif or the take-off SL inhibit formation of the hyper-rotated state (Fig. 4F and fig. S4, C to G).

Last, we tested whether other stalled complexes proceed through a hyper-rotated intermediate. Ribosomes trapped by the stalling motif of the secretion monitor protein (SecM) adopt a rolled conformation similar to that of the gene *60* take-off complexes (*6*, *9*), although the stalling is achieved by a different mechanism (*5*). In the smFRET experiments, SecM-stalled complexes are in the FRET state of 0.7 at low temperature (Fig. 4G). Upon increasing the temperature, a fraction of the SecM-stalled complexes change the conformation to hyper-rotated (Fig. 4H). Thus, the hyper-rotated conformation is sampled by two functionally unrelated types of stalled complexes.

DISCUSSION

Our results suggest how ribosomes can slide along the noncoding mRNA region. Upon reaching the take-off codon, the ribosome slows down (*5*) and pauses at the stop codon in an inactive rolled conformation (*6*). At permissive temperatures, the rolled state is transient and converts into the hyper-rotated state. The rolled conformation may contribute to the observed increased lifetime of nonrotated states as the ribosome reaches the take-off codon (*5*),

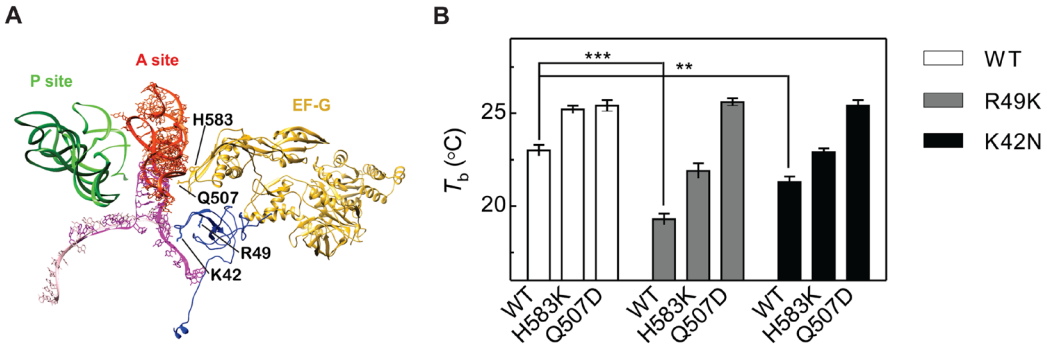

Fig. 3. Ribosomal protein S12 and EF-G tune the temperature dependence. (**A**) Schematic of mutations in S12 and EF-G. Superposition of the structures of a pretranslocation complex with tRNAs in the A and P sites (the tRNAs are red and green, respectively) and EF-G (yellow) (*38*) and of the take-off complex with the P-site peptidyl-tRNA (light green) and the SL in the A-site (purple) (*6*). The position of the A-site SL in the bypassing complex overlaps with the A-site tRNA anticodon domain. Positions of point mutations in EF-G and S12 (dark blue) are indicated. (**B**) The temperatures T_b at which bypassing is half-maximal is shown for the combinations of WT and mutant S12 and EF-G. Error bars show the SD for $n = 3$ replicates. $^{**}P < 0.005$ and $^{***}P < 0.0005$ by Student's two-tailed unpaired *t*-test.

whereas the hyper-rotated state most likely corresponds to the noncanonical long-lived rotated state reported earlier (*5*). The transition into a hyper-rotated state requires the take-off SL in the A site and the nascent peptide in the exit tunnel. These results are in line with previous suggestions that the long pause of the ribosome in a noncanonical state at the take-off site is a hallmark of bypassing induced by the interactions of the nascent peptide (*5*). Recruitment of EF-G–GTP facilitates a pseudotranslocation event using the A-site SL as a tRNA mimic and allows the ribosome to start sliding along mRNA until the landing site is reached. The efficiency of sliding depends on thermally driven conformational transitions at the decoding center and on interactions with the EF-G domain 4. EF-G makes multiple rounds of GTP hydrolysis upon bypassing, with the stoichiometry close to two GTP molecules hydrolyzed per nucleotide of the noncoding gap. The cycles of GTP hydrolysis and Pi release are coupled to EF-G conformational changes that might unlock the ribosome, thereby allowing it to slide along the mRNA, or restrict the backward movement of the ribosome. As the 5′SL elements upstream of the take-off codon emerge from the ribosome, they fold into structures that may prevent the ribosome to move backward (*3*, *6*); GTP hydrolysis by EF-G may further contribute to the directionality of sliding. At the end of the noncoding mRNA gap, ribosome landing is guided by the 3′SL in the mRNA downstream of the landing codon (*3*). When the landing codon is presented in the P site, peptidyl-tRNA^{Gly} engages in the anticodon-codon interaction. Upon landing and EF-G departure, the ribosome adopts a rotated conformation, confirming the previous finding that, at the landing site, the next tRNA accommodates into the rotated ribosome (*5*). After peptide bond formation and subsequent translocation, the ribosome returns into a canonical nonrotated state. The ribosome can now resume translation in the second ORF. Ribosome dynamics during bypassing, with the ribosome going through an unusual hyper-rotated intermediate, is quite different from the cyclic movements between rotated and nonrotated states during canonical translocation, where each cycle of EF-G binding and GTP hydrolysis moves the ribosome by one codon.

The mechanism by which EF-G promotes sliding on gene *60* may provide a general explanation as to how ribosomes move through noncoding parts of mRNAs, such as 3′ untranslated regions of eukaryotic mRNAs (*10*, *11*). These comparisons between the prokaryotic and eukaryotic ribosomes are pertinent because ribosome sliding requires the most conserved elements of the translational machinery, such as the decoding center of the ribosome and EF-G. Our previous results suggested that pausing ribosomes may form short SL structures within the A site (*6*). It would be interesting to see whether these structures form also when ribosomes stall during canonical translation and whether, in some cases, these potential structures are translocated, rather than unwound before translation can resume. Last, the hyper-rotated state of the ribosome appears in both gene *60*– and (unrelated) SecM-stalled ribosomes. A similar hyper-rotated state has been observed for ribosomes pausing at the regulatory SL element of dnaX mRNA (*28*). Thus, the hyper-rotated conformation is likely to be a characteristic feature of stalled complexes before resuming translation. In summary, our results provide the mechanism for unconventional EF-G–promoted movements of the ribosome through the noncoding regions on the mRNA and suggest several new modes of ribosome dynamics that are potentially applicable in prokaryotic and eukaryotic translation.

MATERIALS AND METHODS

Buffer and reagents

All experiments were carried out in HiFi buffer [50 mM tris-HCl (pH 7.5), 70 mM NH_4Cl, 30 mM KCl, 3.5 mM $MgCl_2$, 8 mM putrescine, and 0.5 mM spermidine) (*3*). Chemicals were from Roche Molecular Biochemicals, Sigma-Aldrich, or Merck, and nucleotide triphosphates were from Jena Bioscience. Radioactive compounds were from Hartmann Analytic. Total *Escherichia coli* tRNA was from Roche Molecular Biochemicals. EF-Tu, initiation factors, [^{3}H]Met-tRNA^{fMet}, f[^{3}H]Met-tRNA^{fMet}, and BODIPY-[^{3}H]Met-tRNA^{fMet} were prepared from *E. coli* as described (*3*). Site-directed mutagenesis of the gene *60* construct (*29*) was performed using the QuickChange polymerase chain reaction (PCR) protocol (*3*). The sequence of the SecM mRNA construct was ATTAATACGACTCACTATAGGGGAATTGTGAGCGGATA-ACAATTCCCCTCTAGAAATAATTTTGTTTAACTTTA-AGAAGGAGATATACATATGGAATATCAACACTGGTTAC-GTGAAGCAATAAGCCAACTTCAGGCGAGCGAAAGCCCG-CGGCGTGATGCTGAAATCCTGCTGGAACATGTTACCGG-CAAAGGGCGTACTTTTATCCTCGCCTTTGGTGAAACG-CAGCTGACTGACGAACAATGTCAGCAACTTGATGCGC-TACTGACACGTCGTCGCGATGGTGAACCCATTGCT-CATTTAACCGGGGTGCGAGAATTCTGGTCGTTGCCGT-

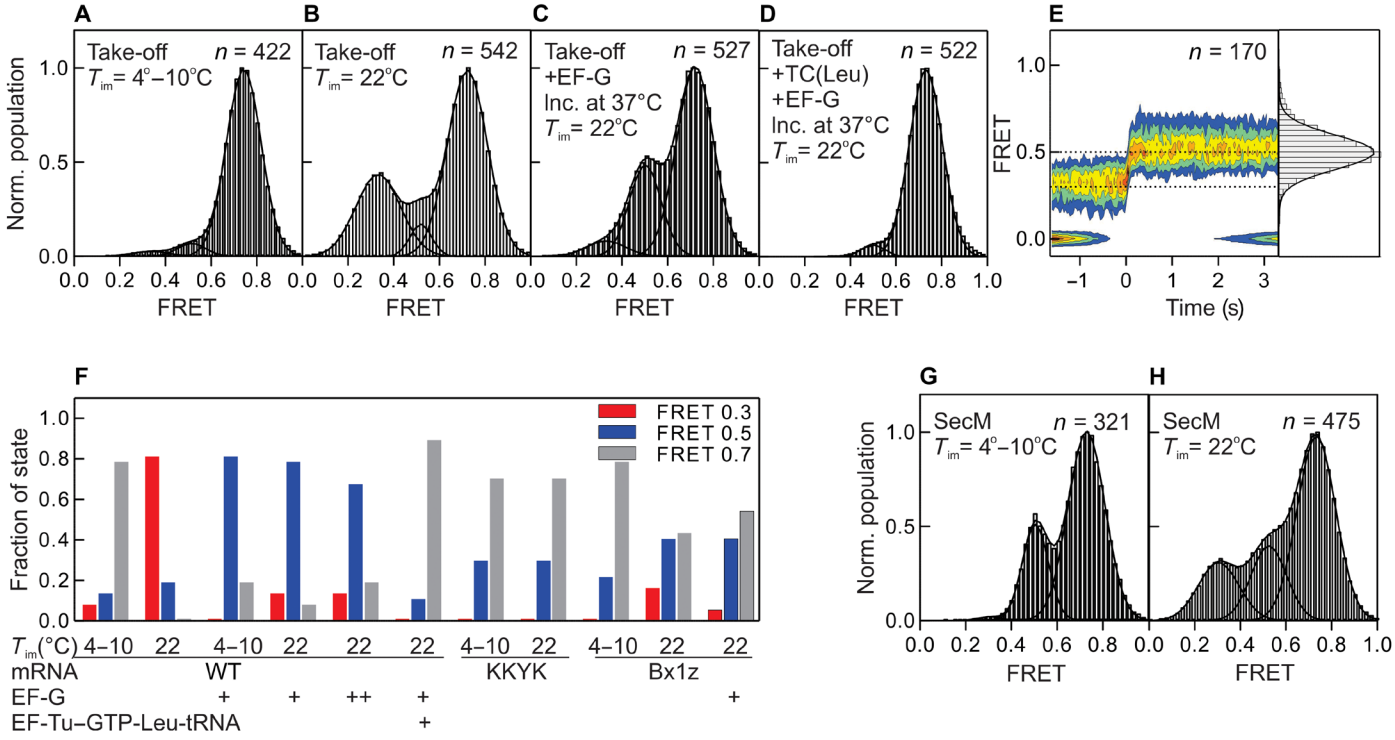

Fig. 4. Ribosome conformation during bypassing visualized by smFRET. (**A** and **B**) FRET distribution histogram for the purified take-off complexes at 4° to 10°C and 22°C, respectively. Black lines indicate the positions of main ribosome populations with FRET efficiencies of 0.3, 0.5, and 0.7 (for statistics, see table S1). T_{im} is the imaging temperature. (**C**) Landing complex obtained by incubation of the take-off complex with EF-G (1 μM) and with GTP for 1 min at 37°C and imaged at 22°C. (**D**) Ribosome conformation after addition of EF-G–GTP and EF-Tu–GTP–Leu-tRNA at 37°C; imaging was at 22°C. (**E**) Time-resolved smFRET recorded upon addition of EF-G (10 nM) with GTP to the imaging buffer. Time courses were synchronized at the first observed transition. Contour plot represents transitions from FRET states of 0.3 to 0.5; other types of transitions were not observed. (**F**) Distribution of hyper-rotated, rotated, and nonrotated conformations in different complexes normalized to the activity of the take-off complex. (**G** and **H**) FRET distribution histograms for the SecM-stalled ribosome complexes at 4° to 10°C and 22°C.

TATTCAGCACGCCCGTCTGGATAAGCCAGGCG-CAAGGCATCCGTGCTGGCCCTATGTCCGGTA-AAATGACTGGTATCGTAAAATGGTTCAACGCTG-ACAAAGGCTTCGGCTTCATCACTCCT. mRNAs were produced by T7 RNA polymerase in vitro transcription and purified by ion exchange chromatography on a HiTrap Q HP 5-ml column (GE Healthcare).

Cloning, expression, and purification of EF-G and EF-G mutants

EF-G mutations H583K and Q507D were introduced by site-directed mutagenesis into pET24EF-G plasmid containing *E. coli* EF-G gene with a C-terminal His-tag. All constructs were verified by DNA sequencing. EF-G wild-type, EF-G(H583K), and EF-G(Q507D) were expressed in BL21(DE3) and purified as described (*30*). Concentrations were determined spectrophotometrically at 280 nm and based on SDS–polyacrylamide gel electrophoresis and densitometry using a reference protein of known concentration.

Ribosomes

Ribosomes (70*S*) were prepared from *E. coli* according to the published protocol (*31*). Fluorescence labeling of ribosomal subunits is described in detail (*24*). The extent of subunit labeling was determined spectroscopically and was close to 100%, and the activity was tested as reported (*24*, *32*). Mutations in the ribosomal protein S12 were introduced into the chromosome-encoded rpsL (ribosomal protein uS12) gene in *E. coli* strain MDS57 (*33*). The genomic region containing the gene was PCR-amplified as two overlapping sections to simultaneously clone and introduce mutations. The R49K mutation was introduced using primer pairs MDP_AEQ and MDP_AER and MDP_AES and MDP_AER, generating strain MDP_224. The K42N mutation was introduced using primer pairs MDP_AEQ and MDP_AEX and MDP_AEW and MDP_AER, generating strain MDP_232. The plasmid pKO3 (*34*) was PCR-amplified with primers MP527 and MP528. Each set of three PCR products was assembled into a circular plasmid using Gibson Assembly (*35*), and the scarless genomic modifications were generated by two-step homologous recombination. The following primers were used:

MDP_AEQ, GCGGTATTGGTAGTCCCACAACACCGTAG-GGATTTACCTTAAGCGGACTT;

MDP_AER, CGTCTATTGAATCGGAGCACCCACAGTCAC-CGGTGTAGAACAGAATACG;

MDP_AES, GAACTCCGCGCTGAAGAAAGTATGCCGT-GTTCGTCTGACTAACGGTTTCG;

MDP_AET, CCGTTAGTCAGACGAACACGGCATACTTT-CTTCAGCGCGGAGTTCGGTTT;

MDP_AEW, TGTATATACTACCACTCCTAACAAACCGA-ACTCCGCGCTGCGTAAAGTAT;

MDP_AEX, TTCGGTTTGTTAGGAGTGGTAGTATATA-CACGAGTACATACGCCACGTTT;

MP527, ACTGTGGGTGCTCCGATTCAATAGACGGA-TCCTCTAGAGTCGACCGGAGA;

MP528, TACGGTGTTGTGGGACTACCAATACCGCGGCCGCGATCCCCGGGTACCGA.

Beginning with a single colony, a 50-ml culture was grown overnight at 37°C with shaking in LB medium without antibiotics. The following day, 1 ml was transferred into each of 12 500 ml of LB medium in flasks (6 liters in total) and grown for ~24 hours at 37°C with shaking in LB medium. The following day, the cells were centrifuged for 10 min at 4000 rpm in 1-liter buckets, resuspended and combined in 500 ml of fresh LB medium at 37°C, and allowed to grow with shaking for 1 hour at 37°C. The cells were then centrifuged 10 min at 4000 rpm in a 1-liter bucket. The cells were washed once with buffer A [20 mM Tris-Cl (pH 7.5), 100 mM KCl, and 15 mM $MgCl_2$], and the pellet was either frozen in liquid nitrogen or directly resuspended in ~100 ml of ice-cold buffer A for lysis. The cells were lysed with a single pass through an EmulsiFlex homogenizer. The lysate was then clarified by (2×) 10-min centrifugation at 13,000 rpm in Falcon tubes. The clarified lysate was then layered on top of a 30-ml cushion of buffer A containing 40% sucrose in Ti45 tubes and centrifuged 17 to 24 hours at 37,000 rpm in a Ti45 rotor. All of the pellets were briefly washed with buffer A and then resuspended in ~500 μl of buffer A (2 to 3 ml in total volume) using small stir bars at 4°C. The resuspended ribosomes were transferred to 1.5-ml tubes, heated to 37°C for 5 min, and then centrifuged at max speed at 4°C in a tabletop centrifuge for 5 min. The supernatant was transferred to fresh tubes, either frozen in liquid nitrogen or diluted to 20 mg/ml, layered on top of 10 to 40% sucrose gradients in buffer A in SW32 tubes (~10 mg ribosomes per gradient; 500 μl), and centrifuged at 22,000 rpm for 17 hours with an SW32 rotor. The gradients were fractionated from the top by hand, in 1-ml fractions, into 1.5-ml tubes. The optical density at 260 nm (OD_{260}) for each fraction was checked and plotted to determine which fractions contained the 70*S* ribosomes. These fractions were combined and centrifuged in a Ti45 rotor 17 to 24 hours at 37,000 rpm. The 70*S* pellets were resuspended in buffer A, and the buffer was exchanged three times using a centrifugal concentrator with a 100,000 molecular weight cutoff. The concentration was adjusted to 8 μM (20 mg/ml), and 50 ml of aliquots was frozen in liquid nitrogen and stored at −80°C.

In vitro translation

Translation was carried out as described (*3*) with the following modifications. Initiation complexes were formed by incubating ribosomes (0.5 μM), mRNA (1.5 μM), IF1, IF2, and IF3 (0.75 μM each), GTP (1 mM), and either BODIPY-[^{3}H]Met-tRNAfMet or initiator f[^{3}H]Met-$tRNA^{fMet}$ (0.5 μM) in HiFi buffer for 30 min at 37°C. The ternary complex EF-Tu–GTP–aminoacyl-tRNA was prepared by incubating EF-Tu (58 μM) with GTP (1 mM), phosphoenol pyruvate (3 mM), and pyruvate kinase (0.1 mg/ml) for 15 min at 37°C, then adding purified total aminoacyl-tRNA (about 60 μM) and EF-G (2 μM), and incubating for 1 min at 37°C. In vitro translation was started by mixing initiation ribosome complexes (0.08 μM) with the ternary complexes (50 μM) with total aminoacyl-tRNA (containing [^{14}C]Leu-$tRNA^{Leu}$) and incubated at temperature ranging from 10° to 37°C for 20 min. Products were separated by Tris-Tricine gel electrophoresis (*36*). Fluorescent peptides were detected after gel electrophoresis using Starion IR/FLA-9000 scanner (Fujifilm) and quantified using the Multi Gauge software. Bypassing efficiency was calculated as a ratio of the density corresponding to the byp band to the sum of the byp and stop bands. The identity of the products was confirmed as previously described (*3*, *6*).

Stalled take-off complexes

To prepare take-off complexes, translation mixtures containing 70*S* ribosomes or fluorescence-labeled 30*S* subunits together with a 1.5-fold excess of labeled 50*S* subunits (0.16 μM) were incubated for 20 min at 10°C, and the resulting ribosome complexes were purified by gel filtration on BioSuite 450 HR 8-μm column (Waters) at 4°C. The amount of the nascent peptide bound to the ribosome was calculated from the ratio f[^{3}H]Met-tRNAfMet radioactivity to OD_{260} in the ribosome fraction.

Leucine incorporation into nascent peptide

Leucine incorporation experiments were performed by mixing stalled take-off complex (0.1 μM) with ternary complex EF-Tu–GTP–[^{14}C]Leu-$tRNA^{Leu}$ (0.3 μM), EF-G (2 μM), and GTP (1 mM) (as indicated). After 2-min incubation at 37°C, samples were quenched with $^1/_2$ volume of 1 M KOH and hydrolyzed for 30 min at 37°C. After neutralization with $^1/_{10}$ volume of acetic acid, the products were analyzed by high-performance liquid chromatography (HPLC) (LiChrospher 100 RP-8 HPLC column, Merck) using an adapted gradient of acetonitrile in 0.1% trifluoroacetic acid.

The GTP hydrolysis assay

The assay was performed by mixing stalled take-off complexes (0.1 μM) with EF-G (0.1 μM) and GTP (10 μM) containing trace amounts of [γ-^{32}P]GTP. Reactions were incubated at 37°C, and aliquots were taken at indicated time intervals and quenched with one volume of 50% formic acid. Samples were analyzed by thin-layer chromatography (Polygram CEL 300, Macherey-Nagel) using a 0.5 M potassium phosphate (pH 3.5) running buffer. Radioactivity was detected using a phosphoimager system. The reaction was carried out under initial velocity conditions, as GTP consumption did not exceed 20% at any reaction point. The extent of bypassing was measured in parallel using the [^{14}C]Leu incorporation assay carried out at exactly the same concentrations as the GTPase assay but with addition of EF-Tu–GTP–[^{14}C]Leu-$tRNA^{Leu}$ (0.3 μM). The bypassing efficiency (20%) is somewhat lower than in all other experiments due to limiting concentrations of EF-G (0.1 μM instead of 2 μM) and GTP (10 μM instead of 1 mM) used in these experiments, which were chosen to maximize the sensitivity of the assay to GTP hydrolysis.

Translocation assay

Translocation with catalytic amounts of EF-G (turnover reaction) and spontaneous translocation in the absence of EF-G were measured using the puromycin assay. Pretranslocation complexes carrying $tRNA^{fMet}$ in the P site and f[^{3}H]Met[^{14}C]Phe-$tRNA^{Phe}$ in the A site were prepared as described (*30*). Pretranslocation complexes (wild type or mutant) (0.1 μM) were incubated with a catalytic amount of EF-G (1 nM) or without EF-G in $TAKM_7$ buffer [50 mM Tris-HCl (pH 7.5) 70 mM NH_4Cl, 30 mM KCl, and 7 mM $MgCl_2$]. Samples were taken and reacted with puromycin (1 mM) for 10 s before being quenched with 1.5 M sodium acetate (pH 4.5) saturated with $MgSO_4$. f[^{3}H]Met[^{14}C]Phe-puromycin was extracted with ethyl acetate and quantified by radioactivity counting. Single-round translocation experiments were carried out in $TAKM_7$ buffer containing 1 mM GTP in a stopped-flow apparatus (SX-20MV, Applied Photophysics) at 37°C. Pretranslocation complexes programmed with an Alexa Fluor 405–labeled mRNA (mMF14Alx405) (0.05 μM) were rapidly mixed with EF-G (4 μM). The dye was excited at 400 nm, and fluorescence was measured after passing a KV418 cutoff filter (Schott).

tRNA stability assay

Pretranslocation complexes with $tRNA^{fMet}$ in the P site and f[^{3}H]Met[^{14}C]Phe-$tRNA^{Phe}$ in the A site were incubated in $TAKM_7$ buffer at 37°C. tRNA binding was assayed by nitrocellulose filtration of the complexes, and the amount of bound tRNA was quantified by radioactive counting.

Single-molecule experiments using TIRF microscopy

Single-molecule FRET experiments were carried out at 22°C or 4° to 10°C temperature as stated. The stalled ribosome complexes were diluted in HiFi buffer to a final concentration of 1 nM and immobilized on biotin–polyethylene glycol quartz slides preincubated with NeutrAvidin (Thermo Fisher Scientific) using the mRNA annealed to a biotinylated primer. The imaging buffer was HiFi containing 3.5 mM $MgCl_2$ supplemented with an oxygen-scavenging system (5 mM protocatechuic acid and 50 nM protocatechuate-3,4-dioxygenase from *Pseudomonas*) and a triplet-state quencher mixture (1 mM Trolox and 1 mM methylviologen) (Sigma-Aldrich), as described (*37*). smFRET experiments were performed on an IX81 inverted objective-based TIRF microscope with a 100× 1.45 numerical aperture oil immersion objective (PLAPON, Olympus). A charge-coupled device C9100-13 camera (Hamamatsu) was used for recording images at a time resolution of 30 frames/s. To image complexes at low temperature, we used an aluminum alloy cube that was cooled on ice and placed on the microscope slide during the measurements. The temperature was controlled and maintained constant within approximately 1°C. Fluorescence time traces for donor (Cy3) and acceptor (Cy5) were extracted and analyzed using custom-made MATLAB (MathWorks) software according to published protocols (*37*). The distribution of FRET states shown in the state histograms was fitted to a sum of Gaussian functions using a nonlinear minimization procedure (fminsearch, MATLAB). The R^2 value for all fits was larger than 0.98. FRET states and corresponding population values were defined from three independent datasets and presented as means ± SD in table S1. For normalization shown in Fig. 4F, we estimated that about 37% of complexes can change the conformation from the nonrotated to either rotated or hyper-rotated under the conditions of the smFRET experiment (Fig. 4B), consistent with the bypassing efficiency (40%) upon temperature shift (Fig. 1C), whereas the remaining fraction remains in the nonrotated state and was omitted from the calculations.

SUPPLEMENTARY MATERIALS

Supplementary material for this article is available at http://advances.sciencemag.org/cgi/content/full/5/6/eaaw9049/DC1

Fig. S1. HPLC separation of the take-off and landing products.

Fig. S2. Temperature dependence of bypassing: The effect of mRNA elements and the nascent peptide.

Fig. S3. The effect of mutations in S12 and EF-G.

Fig. S4. FRET distribution histograms.

Table S1. Summary of the smFRET data.

REFERENCES AND NOTES

1. R. B. Weiss, W. M. Huang, D. M. Dunn, A nascent peptide is required for ribosomal bypass of the coding gap in bacteriophage T4 gene *60*. *Cell* **62**, 117–126 (1990).
2. B. F. Lang, M. Jakubkova, E. Hegedusova, R. Daoud, L. Forget, B. Brejova, T. Vinar, P. Kosa, D. Fricova, M. Nebohacova, P. Griac, L. Tomaska, G. Burger, J. Nosek, Massive programmed translational jumping in mitochondria. *Proc. Natl. Acad. Sci. U.S.A.* **111**, 5926–5931 (2014).
3. E. Samatova, A. L. Konevega, N. M. Wills, J. F. Atkins, M. V. Rodnina, High-efficiency translational bypassing of non-coding nucleotides specified by mRNA structure and nascent peptide. *Nat. Commun.* **5**, 4459 (2014).
4. A. J. Herr, N. M. Wills, C. C. Nelson, R. F. Gesteland, J. F. Atkins, Drop-off during ribosome hopping. *J. Mol. Biol.* **311**, 445–452 (2001).
5. J. Chen, A. Coakley, M. O'Connor, A. Petrov, S. E. O'Leary, J. F. Atkins, J. D. Puglisi, Coupling of mRNA structure rearrangement to ribosome movement during bypassing of non-coding regions. *Cell* **163**, 1267–1280 (2015).
6. X. Agirrezabala, E. Samatova, M. Klimova, M. Zamora, D. Gil-Carton, M. V. Rodnina, M. Valle, Ribosome rearrangements at the onset of translational bypassing. *Sci. Adv.* **3**, e1700147 (2017).
7. A. J. Herr, J. F. Atkins, R. F. Gesteland, Coupling of open reading frames by translational bypassing. *Annu. Rev. Biochem.* **69**, 343–372 (2000).
8. A. J. Herr, R. F. Gesteland, J. F. Atkins, One protein from two open reading frames: Mechanism of a 50 nt translational bypass. *EMBO J.* **19**, 2671–2680 (2000).
9. J. Zhang, X. Pan, K. Yan, S. Sun, N. Gao, S.-F. Sui, Mechanisms of ribosome stalling by SecM at multiple elongation steps. *eLife* **4**, e09684 (2015).
10. T. P. Miettinen, M. Björklund, Modified ribosome profiling reveals high abundance of ribosome protected mRNA fragments derived from 3′ untranslated regions. *Nucleic Acids Res.* **43**, 1019–1034 (2015).
11. N. R. Guydosh, R. Green, Dom34 rescues ribosomes in 3′ untranslated regions. *Cell* **156**, 950–962 (2014).
12. L. K. Doerfel, I. Wohlgemuth, C. Kothe, F. Peske, H. Urlaub, M. V. Rodnina, EF-P is essential for rapid synthesis of proteins containing consecutive proline residues. *Science* **339**, 85–88 (2013).
13. I. Wohlgemuth, C. Pohl, M. V. Rodnina, Optimization of speed and accuracy of decoding in translation. *EMBO J.* **29**, 3701–3709 (2010).
14. A. Savelsbergh, N. B. Matassova, M. V. Rodnina, W. Wintermeyer, Role of domains 4 and 5 in elongation factor G functions on the ribosome. *J. Mol. Biol.* **300**, 951–961 (2000).
15. C. Chen, X. Cui, J. F. Beausang, H. Zhang, I. Farrell, B. S. Cooperman, Y. E. Goldman, Elongation factor G initiates translocation through a power stroke. *Proc. Natl. Acad. Sci. U.S.A.* **113**, 7515–7520 (2016).
16. S. Joseph, B. Weiser, H. F. Noller, Mapping the inside of the ribosome with an RNA helical ruler. *Science* **278**, 1093–1098 (1997).
17. K. Fredrick, H. F. Noller, Accurate translocation of mRNA by the ribosome requires a peptidyl group or its analog on the tRNA moving into the 30S P site. *Mol. Cell* **9**, 1125–1131 (2002).
18. H. Demirci, L. Wang, F. V. Murphy IV, E. L. Murphy, J. F. Carr, S. C. Blanchard, G. Jogl, A. E. Dahlberg, S. T. Gregory, The central role of protein S12 in organizing the structure of the decoding site of the ribosome. *RNA* **19**, 1791–1801 (2013).
19. D. Sharma, A. R. Cukras, E. J. Rogers, D. R. Southworth, R. Green, Mutational analysis of S12 protein and implications for the accuracy of decoding by the ribosome. *J. Mol. Biol.* **374**, 1065–1076 (2007).
20. A. R. Cukras, D. R. Southworth, J. L. Brunelle, G. M. Culver, R. Green, Ribosomal proteins S12 and S13 function as control elements for translocation of the mRNA: tRNA complex. *Mol. Cell* **12**, 321–328 (2003).
21. D. S. Tourigny, I. S. Fernández, A. C. Kelley, V. Ramakrishnan, Elongation factor G bound to the ribosome in an intermediate state of translocation. *Science* **340**, 1235490 (2013).
22. J. Zhou, L. Lancaster, J. P. Donohue, H. F. Noller, Crystal structures of EF-G–ribosome complexes trapped in intermediate states of translocation. *Science* **340**, 1236086 (2013).
23. R. Hickerson, Z. K. Majumdar, A. Baucom, R. M. Clegg, H. F. Noller, Measurement of internal movements within the 30 S ribosomal subunit using Förster resonance energy transfer. *J. Mol. Biol.* **354**, 459–472 (2005).
24. H. Sharma, S. Adio, T. Senyushkina, R. Belardinelli, F. Peske, M. V. Rodnina, Kinetics of spontaneous and EF-G-accelerated rotation of ribosomal subunits. *Cell Rep.* **16**, 2187–2196 (2016).
25. P. V. Cornish, D. N. Ermolenko, H. F. Noller, T. Ha, Spontaneous intersubunit rotation in single ribosomes. *Mol. Cell* **30**, 578–588 (2008).
26. C. Ling, D. N. Ermolenko, Initiation factor 2 stabilizes the ribosome in a semirotated conformation. *Proc. Natl. Acad. Sci. U.S.A.* **112**, 15874–15879 (2015).
27. S. Adio, H. Sharma, T. Senyushkina, P. Karki, C. Maracci, I. Wohlgemuth, W. Holtkamp, F. Peske, M. V. Rodnina, Dynamics of ribosomes and release factors during translation termination in *E. coli*. *eLife* **7**, e34252 (2018).
28. P. Qin, D. Yu, X. Zuo, P. V. Cornish, Structured mRNA induces the ribosome into a hyper-rotated state. *EMBO Rep.* **15**, 185–190 (2014).
29. N. M. Wills, M. O'Connor, C. C. Nelson, C. C. Rettberg, W. M. Huang, R. F. Gesteland, J. F. Atkins, Translational bypassing without peptidyl-tRNA anticodon scanning of coding gap mRNA. *EMBO J.* **27**, 2533–2544 (2008).
30. C. E. Cunha, R. Belardinelli, F. Peske, W. Holtkamp, W. Wintermeyer, M. V. Rodnina, Dual use of GTP hydrolysis by elongation factor G on the ribosome. *Translation (Austin)* **1**, e24315 (2013).
31. M. V. Rodnina, W. Wintermeyer, GTP consumption of elongation factor Tu during translation of heteropolymeric mRNAs. *Proc. Natl. Acad. Sci. U.S.A.* **92**, 1945–1949 (1995).
32. R. Belardinelli, H. Sharma, N. Caliskan, C. E. Cunha, F. Peske, W. Wintermeyer, M. V. Rodnina, Choreography of molecular movements during ribosome progression along mRNA. *Nat. Struct. Mol. Biol.* **23**, 342–348 (2016).

33. G. Posfai, G. Plunkett III, T. Fehér, D. Frisch, G. M. Keil, K. Umenhoffer, V. Kolisnychenko, B. Stahl, S. S. Sharma, M. de Arruda, V. Burland, S. W. Harcum, F. R. Blattner, Emergent properties of reduced-genome *Escherichia coli*. *Science* **312**, 1044–1046 (2006).
34. A. J. Link, D. Phillips, G. M. Church, Methods for generating precise deletions and insertions in the genome of wild-type Escherichia coli: Application to open reading frame characterization. *J. Bacteriol.* **179**, 6228–6237 (1997).
35. D. G. Gibson, L. Young, R.-Y. Chuang, J. C. Venter, C. A. Hutchison, H. O. Smith, Enzymatic assembly of DNA molecules up to several hundred kilobases. *Nat. Methods* **6**, 343–345 (2009).
36. H. Schägger, G. von Jagow, Tricine-sodium dodecyl sulfate-polyacrylamide gel electrophoresis for the separation of proteins in the range from 1 to 100 kDa. *Anal. Biochem.* **166**, 368–379 (1987).
37. S. Adio, T. Senyushkina, F. Peske, N. Fischer, W. Wintermeyer, M. V. Rodnina, Fluctuations between multiple EF-G-induced chimeric tRNA states during translocation on the ribosome. *Nat. Commun.* **6**, 7442 (2015).
38. A. F. Brilot, A. A. Korostelev, D. N. Ermolenko, N. Grigorieff, Structure of the ribosome with elongation factor G trapped in the pretranslocation state. *Proc. Natl. Acad. Sci. U.S.A.* **110**, 20994–20999 (2013).

Acknowledgments: We thank H. Sharma for providing fluorescence-labeled ribosomal subunits; M. Liutkute for providing the SecM mRNA, N. Korniy for UUA-specific $tRNA^{Leu}$, and O. Geintzer, V. Herold, S. Kappler, C. Kothe, A. Pfeifer, T. Uhlendorf, T. Wiles, F. Hummel, and M. Zimmermann for expert technical assistance. **Funding:** This research was supported by the Max Planck Society and a grant of the Deutsche Forschungsgemeinschaft (SFB860) and the Leibniz Prize of the Deutsche Forschungsgemeinschaft. M.K. is a recipient of the Excellence Fellowship of the Göttingen Graduate School for Neurosciences, Biophysics, and Molecular Biosciences. **Author contributions:** M.K. and E.S. designed and performed biochemical experiments, analyzed data, and wrote the manuscript. T.S. performed all smFRET experiments, analyzed data, and contributed to writing the manuscript. B.Z.P. conducted experiments and analyzed data. M.P. designed and prepared mutant ribosomes. E.S., F.P., and M.V.R. supervised the project and contributed to the interpretation of the work and to writing the manuscript. **Competing interests:** The authors declare that they have no competing interests. **Data and materials availability:** All data needed to evaluate the conclusions in the paper are present in the paper and/or the Supplementary Materials. Additional data related to this paper may be requested from the authors.

Submitted 5 February 2019
Accepted 25 April 2019
Published 5 June 2019
10.1126/sciadv.aaw9049

Citation: M. Klimova, T. Senyushkina, E. Samatova, B. Z. Peng, M. Pearson, F. Peske, M. V. Rodnina, EF-G–induced ribosome sliding along the noncoding mRNA. *Sci. Adv.* **5**, eaaw9049 (2019).